

Distinguishing scalar from pseudoscalar Higgs production at the LHC

B. Field*

*C.N. Yang Institute for Theoretical Physics, Stony Brook University, Stony Brook, New York 11794-3840, USA and
Department of Physics, Brookhaven National Laboratory, Upton, New York 11973, USA*

(Dated: August 29, 2002)

In this letter we examine the production channels for the scalar or pseudoscalar Higgs plus two jets at the CERN Large Hadron Collider (LHC). We identify possible signals for distinguishing between a scalar and a pseudoscalar Higgs boson.

PACS numbers: 13.85.-t, 14.80.Bn, 14.80.Cp

I. INTRODUCTION

The Higgs mechanism is responsible for electroweak symmetry breaking in the Standard Model (SM). The experimental lower limit on the Higgs mass is approximately 114 GeV[1]. There are many models that contain more than one Higgs boson in various numbers of doublets. In the Minimal Supersymmetric Standard Model (MSSM) there are two Higgs doublets that give five physical Higgs bosons: two neutral (H_1^0, H_2^0), two charged H^\pm , and one neutral pseudoscalar A (for review see [2]). In the MSSM the mass limits change slightly with the lightest of the two neutral scalars H_1^0 (afterwards referred to as simply H) having a mass greater than about 91 GeV and the pseudoscalar being more massive than roughly 92 GeV[3].

Finding one or more Higgs bosons is the top priority of high energy physics programs around the world. A subset of Higgs bosons in some doublet models may be experimentally difficult to distinguish. The characteristics of the scalar H and pseudoscalar A Higgs boson within the MSSM are of particular interest.

We study the production of both the scalar and pseudoscalar Higgs in association with two jets in hadron collisions. At the LHC the primary processes that produce a Higgs plus two jets are $gg \rightarrow ggH$ and $qg \rightarrow qgH$, accounting for approximately 60%(40%) of the total cross-section respectively. The same is true for the production of the pseudoscalar. Other channels that contribute to the total cross-section include $qg \rightarrow ggH$ and $qg \rightarrow qgH$, although these channels have been shown to add very little to the total cross-section. Total cross-sections of the scalar and pseudoscalar exist[4, 5, 6] at the lowest order and differential cross-sections for the scalar case are also available[7, 8]. In the following calculations, only the two dominant channels were considered as the other channels are negligible.

In this letter, we propose a technique for distinguishing between a scalar and a pseudoscalar Higgs when produced in association with two jets by means of a splitting that occurs in a specific integrated operator moment. This distinction is important both experimentally and theoretically in order to separate the two kinds of events and understand the properties of these particles which would otherwise be very difficult due to the similarity in their physical observables.

II. EFFECTIVE LAGRANGIAN

We work in the limit that the top quark is much heavier than the Higgs boson[9], integrating out the top quark and neglecting all the other quarks that would normally appear in the loop diagrams. This has been shown to be an excellent approximation and remains very good even when the Higgs mass is heavier than the mass of the top quark. In general this approximation is considered to be a good one when $M_{H,A} < 2m_t$. We consider Higgs bosons lighter than 200 GeV. The effective Lagrangian used in the scalar case is defined as

$$\mathcal{L}_{\text{eff}}^H = -\frac{1}{4}g_H H G_{\mu\nu}^a G^{a,\mu\nu} \quad (1)$$

where $g_H = \alpha_s/3\pi v$. $G_{\mu\nu}^a$ is the field-strength tensor for the gluons. The vacuum expectation value (vev) of the Higgs field is determined in the usual way as $v^2 = (\sqrt{2}G_F)^{-1}$ and is numerically equal to approximately 246 GeV. For the pseudoscalar case we let the Higgs couple to the quarks with a γ_5 and the effective Lagrangian can be written as

$$\mathcal{L}_{\text{eff}}^A = g_A A G_{\mu\nu}^a \tilde{G}^{a,\mu\nu} \quad (2)$$

*bfield@ic.sunysb.edu

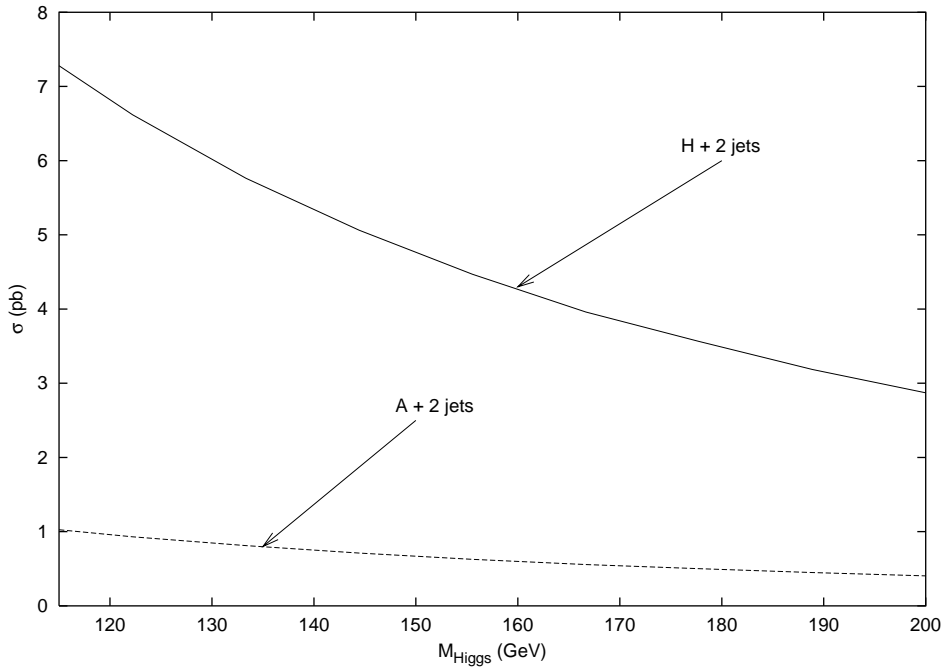


FIG. 1: Total cross-sections for scalar and pseudoscalar Higgs plus two jets. These curves are for the LHC with the cuts described in the text.

where $g_A = \alpha_s/8\pi v$. Here $\tilde{G}_{\mu\nu}^a = 1/2\epsilon^{\mu\nu\rho\sigma}G_{\rho\sigma}^a$ is the dual of the gluon field-strength tensor.

This effective Lagrangian generates a scalar Higgs coupling to two, three, and four gluons or a pseudoscalar coupling to two or three gluons. The four gluon coupling to a pseudoscalar vertex vanishes via the Jacobi identity as it is proportional to a completely antisymmetric combination of structure constants. The Feynman rules for these effective theories can be found in [4] (for the scalar) and [5] (for the pseudoscalar).

III. OBSERVABLES AND MOMENTS

We present our results for the LHC with $\sqrt{S} = 14$ TeV. We have used the CTEQ6L parton distribution functions[10] with $\Lambda_5^{\text{LO}} = 226$ MeV with a one-loop running of α_s for consistency with a value of $\alpha_s(M_Z) = 0.137$. The transverse momentum (p_t) was constrained to be more than 25 GeV for the Higgs and each of the two jets. Also the rapidity was constrained to be $|y| < 2.5$ for all the outgoing particles. The separation of the jets was restricted to be $\Delta R \equiv \sqrt{\Delta\phi^2 + \Delta\eta^2} \geq 0.7$.

The total cross-section of these two channels are shown in Fig. 1. These cross-sections agree exactly with those in the literature[4, 5]. When plotted in this linear fashion it is interesting to note the differences in the dependence of the cross-sections on the mass of the Higgs boson. Both total cross-sections loose more than two-thirds of their value from 100 – 200 GeV and appear in the approximate ratio of $(g_H/g_A)^2 = 9/64$ due to the similarity in their matrix elements.

Fig. 2 shows the normalized transverse momentum spectrum of both the production channels. The pseudoscalar Higgs p_t spectrum was displaced down by 10% to allow the two curves to be distinguished. If this had not been done, the curves would lie virtually on top of one another. Fig. 3 shows the center-of-momentum angle between the Higgs and the highest p_t jet for the two reactions. This shows what would be expected naively, that the Higgs prefers to come out back-to-back with the highest p_t jet. Once again, the pseudoscalar curve has been scaled down by 20% to allow both curves to be seen clearly. No significant differences between these curves were found.

The authors of [11] presented a technique for determining the CP nature of the Higgs boson in $t\bar{t}H$ production based on certain weighted moments of the cross-section. The cross-section integral was weighted by operators \mathcal{O}_{CP} . The six operators presented in [11] are scalar and cross products of the momentum of the outgoing particles (in this case the massive top quarks). We propose using the same test for the massless quarks and gluons that make up the jets. All of these weighted moments were examined as well as some novel ones and the only operator from these sets

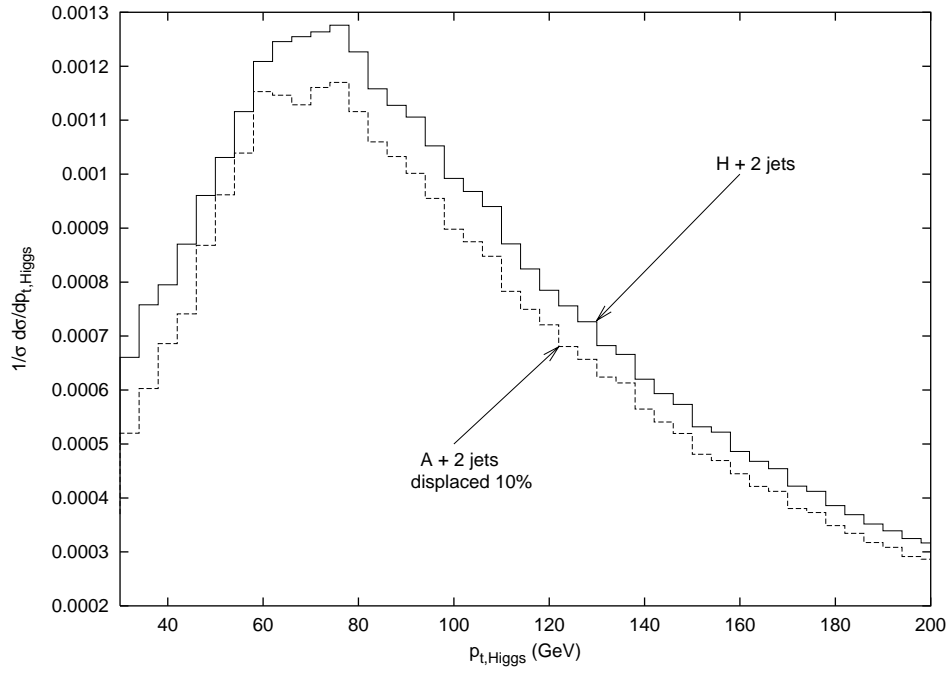


FIG. 2: Normalized transverse momentum spectrum of the scalar or pseudoscalar Higgs production channels plus two jets. The Higgs mass for both the scalar and pseudoscalar is 120 GeV. Note that the pseudoscalar Higgs has been displaced down by 10% to allow the two curves to be distinguished. These curves are for the LHC with the cuts described in the text.

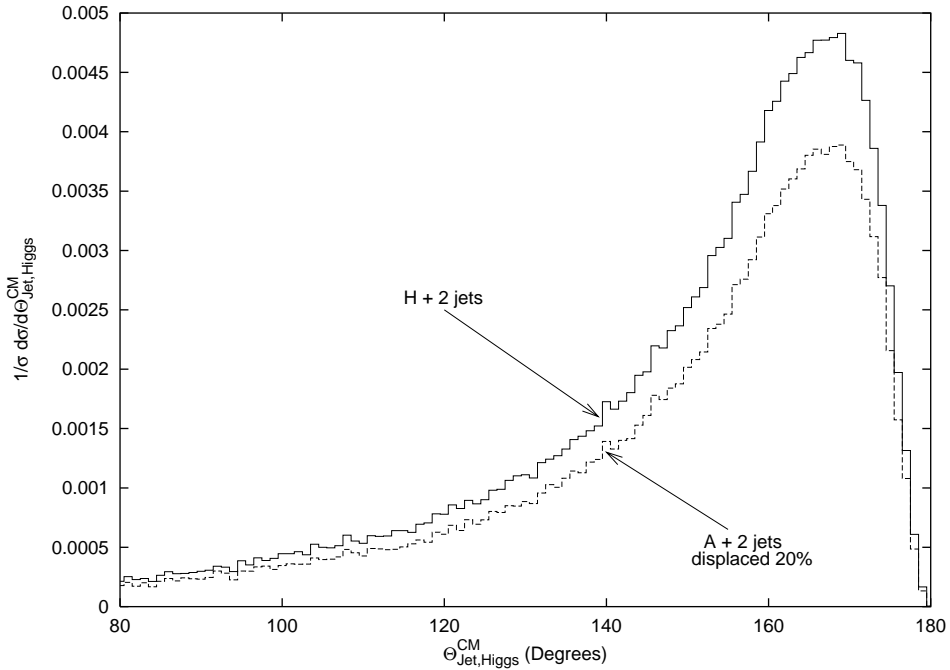


FIG. 3: Normalized opening angle in the center-of-momentum frame between the Higgs and the highest p_t jet for the scalar and pseudoscalar Higgs production channels plus two jets. The Higgs mass for both the scalar and pseudoscalar is 120 GeV. Note that the pseudoscalar Higgs has been displaced down by 20% to allow the two curves to be distinguished. These curves are for the LHC with the cuts described in the text.

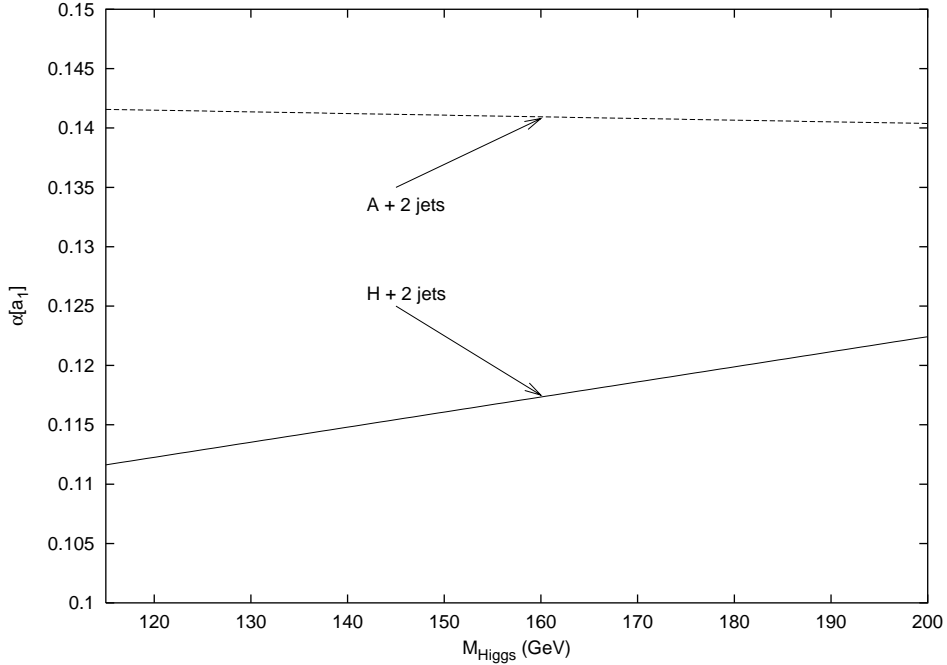


FIG. 4: Normalized integrated moment $\alpha[a_1]$ for the scalar and pseudoscalar Higgs plus two jets. The splitting between the two different production channels is clear at all mass scales. These curves are for the LHC with the cuts described in the text.

that produced a significant difference between the scalar and the pseudoscalar signals was the operator[11]

$$a_1 = \frac{(\vec{p}_1 \times \hat{z}) \cdot (\vec{p}_2 \times \hat{z})}{|(\vec{p}_1 \times \hat{z}) \cdot (\vec{p}_2 \times \hat{z})|} \quad (3)$$

when it was integrated and normalized as prescribed below

$$\alpha[\mathcal{O}_{CP}] \equiv \frac{1}{\sigma} \int \mathcal{O}_{CP} d\sigma dPS \quad (4)$$

where p_1 and p_2 are the momentum of the two jets and \hat{z} is the axis of the beam. The a_1 operator is sensitive to the cosine of the angle between the transverse momentum vectors of the two jets. Distinguishing between the two jets is not important as this moment is invariant under $1 \leftrightarrow 2$. Another combination of momentum in the above equations that was considered was to use the moment operators presented in [11] with $p_1 = p_{\text{Higgs}}$ and p_2 the momentum of the highest p_t jet. However, this yielded no differences in the integrated moments making this definition of little use for these channels.

Fig. 4 shows the results of this integration as a function of the Higgs mass. This integrated moment showed a modest splitting at all Higgs mass scales from 100 – 200 GeV. The pseudoscalar does not show much mass dependence. However, the scalar integrated moment rises slightly with increasing Higgs mass. This effect might also be useful as another method for constraining the mass of the scalar Higgs boson. The splitting in Fig. 4 helps to remove the problems created by the degeneracy in the physical observable of the scalar and the pseudoscalar. If the two signals could not be separated, the doublet structure of the model would not be easily measured. In the case of the MSSM this would mean that part of the supersymmetric signal might be lost or the mass of the scalar Higgs may be determined incorrectly if the pseudoscalar events were wrongly identified as scalar events.

Separating the two signals is theoretically intriguing because it appears to be one of the only ways to predict a difference between the scalar and pseudoscalar events of this nature at the LHC by means other than the magnitude of their cross-section. This is also interesting experimentally as it leads to the possibility of separating the two kinds of Higgs events with the added bonus that the z momentum is not needed in this analysis.

IV. CONCLUSIONS

The production channels of the scalar or pseudoscalar Higgs plus two jets were found to have many similarities in their physical observables and one important difference in the integrated moment $\alpha[a_1]$. This may help to reduce the

difficulty in distinguishing between the two types of events at the LHC. The most important aspect of separating the two signals is to make sure that the doublet structure (the supersymmetric signal in the case of the MSSM) is not lost because of its small cross-section and its similarity to the scalar Higgs with respect to its physical observables or wrongly determining the mass of the scalar Higgs by misidentifying pseudoscalar events as scalar events. The proposed technique presented in this letter may enable these two signals to be separated after a full detector simulation is preformed.

APPENDIX A: DIFFERENCES IN THE AMPLITUDES

It turns out that the differences in the scalar (or pseudoscalar) plus two jets amplitudes squared were very small. The differences will be presented in using the helicity basis presented in [4, 5] to make for the most compact matrix elements squared. These matrix elements have been found to be in exact analytic agreement with the four dimentional matrix elements presented in [7]. We identify the momentum as follows (where X should be considered the Higgs for the process in question, playing the part of either the scalar or the pseudoscalar). All the momentum are outgoing.

$$q(p_1) + \bar{q}(p_2) \rightarrow g(-p_3) + g(-p_4) + X(-p_5) \quad (A1)$$

$$g(p_1) + g(p_2) \rightarrow g(-p_3) + g(-p_4) + X(-p_5) \quad (A2)$$

$$q(p_1) + \bar{q}(p_2) \rightarrow q(-p_3) + \bar{q}(-p_4) + X(-p_5). \quad (A3)$$

In the following we define $S_{ab} = (p_a + p_b)^2 = 2p_a \cdot p_b$. Color factors have been included in the expression for the $qqggH(A)$ and $qqqqH(A)$ channels as they affect the terms differently but not in the expression for the $ggggH(A)$ channel as there is one overall color factor for all the matrix elements squared. Here N is the number of colors. Color and spin averages have not been included nor have any coupling constants.

For the $qqggH(A)$ channel the difference in the scalar minus the pseudoscalar amplitude squared was 15 terms out of 626. Setting the color factors to match those presented in [7], $C_O = (N^2 - 1)/N$ and $C_K = (N^2 - 1)N$ the difference was found to be

$$\begin{aligned} |\mathcal{M}|_{qq \rightarrow ggH}^2 - |\mathcal{M}|_{qq \rightarrow ggA}^2 &= 2C_K - 6C_O \\ &+ \left(\left\{ \frac{4C_O}{S_{12}^2 S_{34}^2} \left[S_{13} S_{14} S_{23} S_{24} - S_{13}^2 S_{24}^2 \right] + 4C_O \frac{S_{13} S_{24}}{S_{12} S_{34}} \right. \right. \\ &\quad \left. \left. \frac{1}{S_{13} S_{24}} \left[C_O (S_{12} S_{34} - S_{14} S_{23}) + C_K (S_{14} S_{23} - S_{12} S_{34}) \right] \right\} + \{3 \leftrightarrow 4\} \right). \end{aligned} \quad (A4)$$

For the $ggggH(A)$ channel the difference in the scalar minus the pseudoscalar was 16 terms out of 2761. The overall color factor is $N^2(N^2 - 1)$. The difference was

$$\begin{aligned} |\mathcal{M}|_{gg \rightarrow ggH}^2 - |\mathcal{M}|_{gg \rightarrow ggA}^2 &= 48 + \left(8 \left\{ \frac{1}{2} \frac{1}{S_{12}^2 S_{34}^2} \left[S_{13} S_{24} - S_{14} S_{23} \right]^2 - \frac{1}{2} \frac{1}{S_{12} S_{34}} \left[S_{13} S_{24} + S_{14} S_{23} \right]^2 \right. \right. \\ &\quad \left. \left. + \frac{1}{S_{13}^2 S_{24}^2} \left[S_{12} S_{34} - S_{14} S_{23} \right]^2 - \frac{1}{S_{13} S_{24}} \left[S_{12} S_{34} + S_{14} S_{23} \right] \right\} + \{3 \leftrightarrow 4\} \right). \end{aligned} \quad (A5)$$

Finally, there are two cases for the $qqqqH(A)$ amplitude squared. If there are identical quarks allowed in the scattering process ($q\bar{q}q\bar{q}H(A)$) then there are two diagrams that contribute. The color factors here are $C_A = N$ and $C_F = (N^2 - 1)/2N$. The difference in the amplitudes squared is 19 out of 39 terms and is equal to

$$|\mathcal{M}|_{qq \rightarrow qqH}^2 - |\mathcal{M}|_{qq \rightarrow qqA}^2 = 4C_A C_F \left(2 - \frac{4}{C_A} + \frac{(S_{13} S_{24} - S_{14} S_{23})^2}{S_{12}^2 S_{34}^2} + \frac{(S_{14} S_{23} - S_{12} S_{34})^2}{S_{13}^2 S_{24}^2} \right) \quad (A6)$$

$$- 2 \frac{S_{13} S_{24}}{S_{12} S_{34}} - 2 \frac{S_{12} S_{34}}{S_{13} S_{24}} + \frac{2}{C_A} \left(\frac{S_{12} S_{32} - S_{14} S_{23}}{S_{13} S_{24}} \right) + \{3 \leftrightarrow 4\}. \quad (A7)$$

If a different quark pair is created ($q\bar{q}q'\bar{q}'H(A)$), then the difference is smaller as only one diagram is needed for the amplitude. Here 6 out of 10 terms survive and are equal to

$$|\mathcal{M}|_{qq \rightarrow qqH}^2 - |\mathcal{M}|_{qq \rightarrow qqA}^2 = 4C_F \left(1 + \left\{ \frac{(S_{13} S_{24} - S_{13} S_{24})^2}{S_{12}^2 S_{34}^2} - \frac{S_{13} S_{24} + S_{14} S_{23}}{S_{12} S_{34}} \right\} + \{3 \leftrightarrow 4\} \right). \quad (A8)$$

It should also be noted that all these differences are invariant under $1 \leftrightarrow 2$.

ACKNOWLEDGMENTS

The author would like to thank J. Smith, S. Dawson, R.P. Kauffman, S.V. Desai, W. Kilgore, F. Paige, and J. Laiho for their help and comments on this paper at all stages of its development. The author was partially supported by the National Science Foundation grant PHY-0098527 and the U.S. Department of Energy under Contract No. DE-AC02-98CH10886.

- [1] R. Barate *et al.* (ALEPH Collaboration), Phys. Lett. **B495** 1 (2000)
 M. Acciarri *et al.* (L3 Collaboration), Phys. Lett. **B495** 18 (2000)
 P. Abreu *et al.* (DELPHI Collaboration), Phys. Lett. **B499** 23 (2001)
 G. Abbiendi *et al.* (OPAL Collaboration), Phys. Lett. **B499** 38 (2001).
- [2] J.F. Gunion, H.E. Haber, G.L. Kane, and S. Dawson, “This Higgs Hunter’s Guide”, (Addison-Wesley, Reading, MA, 1990), Erratum *ibid.* hep-ph/9302272.
- [3] ALEPH Collaboration, DELPHI Collaboration, L3 Collaboration, OPAL Collaboration, LEP Higgs Working Group, hep-ex/0107030.
- [4] R.P. Kauffman, S.V. Desai, and D. Risal, Phys. Rev. D **55** 4005 (1997), hep-ph/9610541, Erratum *ibid.* Phys. Rev. D **58** 119901 (1998). Further typos were found and corrected in Ref. [7].
- [5] R.P. Kauffman and S.V. Desai, Phys. Rev. D **59** 057054 (1999), hep-ph/9808286.
- [6] V. Del Duca, W. Kilgore, C. Oleari, C. Schmidt, and D. Zeppenfeld, Nucl. Phys. **B616** 367 (2001), hep-ph/0108030 and references therein.
- [7] V. Ravindran, J. Smith, and W.L. van Neerven, Nucl. Phys. **B634** 247 (2002), hep-ph/0201114.
- [8] D. de Florian, M. Grazzini, and Z. Kunszt, Phys. Rev. Lett. **82** 5209 (1999), hep-ph/9902483.
- [9] For the scalar Higgs see A. Vainshtein, M. Voloshin, V. Zakharov, and M. Shifman, Sov. J. Nucl. Phys. **30** 429 (1979); S. Dawson, Nucl. Phys. **B359** 283 (1991); A. Djouadi, M. Spira, and P.M. Zerwas, Phys. Lett. **B264** 440 (1991); B.A. Kniehl and M. Spira, Z. Phys. **C69** 77 (1994), hep-ph/9505225. For the pseudoscalar Higgs see R.P. Kauffman and W. Schaffer, Phys. Rev. D **49** 551 (1994), hep-ph/9305279.
- [10] J. Pumplin, D.R. Stump, J. Huston, H.L. Lai, P. Nadolsky, and W.K. Tung, JHEP **0207** 012 (2002), hep-ph/0201195.
- [11] J.F. Gunion and X.-G. He, Phys. Rev. Lett. **76** 4468 (1996), hep-ph/9602226.